UC Davis

UC Davis Previously Published Works

Title

Single-Site Osmium Catalysts on MgO: Reactivity and Catalysis of CO Oxidation

Permalink

https://escholarship.org/uc/item/89h708nr

Journal

Chemistry - A European Journal, 23(11)

ISSN

0947-6539

Authors

Yang, Dong

Zhang, Shengjie

Xu, Pinghong

et al.

Publication Date

2017-02-21

DOI

10.1002/chem.201605131

Peer reviewed

eScholarship.org Powered by the California Digital Library
University of California

Single-site osmium catalysts on MgO: reactivity and catalysis of CO oxidation

Dong Yang,[a] Shengjie Zhang,[b] Pinghong Xu,[a] Nigel D. Browning,[c] David A. Dixon,*[b] Bruce C.

ChemSusChem Communications

Abstract: MgO-supported osmium dioxo species described as $Os(=O)_2\{-O_{support}\}_{1or2}$ (the braces denote O atoms of the MgO surface) formed from $Os_3(CO)_{12}$ via supported $Os(CO)_2$ and characterized by spectroscopy, microscopy, and theory react with ethylene at 298 K to form osmium glycol species or with CO to give osmium mono- and di-carbonyls. $Os(=O)_2\{-O_{support}\}_{1or2}$ is the precursor of a CO oxidation catalyst characterized by a turnover frequency of 4.0×10^{-3} (molecules of CO)/(Os atom × s) at 473 K; the active species are inferred to be osmium monocarbonyls. The structures and frequencies calculated at the level of density functional theory with the B3LYP functional bolster the experimental results and facilitate structural assignments. The lowest-energy structures have various osmium oxidation and spin states. The results demonstrate not only new chemistry of the supported single-site catalysts but also their complexity and the value of complementary techniques used in concert to unravel the chemistry.

Metals dispersed atomically on supports are drawing wide attention because they offer new catalytic properties and the benefit of maximum accessibility of the metal.[1] Examples include oxide-supported noble metals Au,[2] Pt,[3] and Ir.[4] Questions about these catalysts include those focused on the metal oxidation state, ligands (including the support), and resistance to metal aggregation. Demonstrations of site isolation require imaging of the metal atoms (e.g., by scanning transmission electron microscopy (STEM) of heavy metal atoms on supports comprising light atoms for good contrast).

Because mononuclear osmium complexes in solution have a rich chemistry (e.g., asymmetric catalytic oxidation of olefins[5]) involving Os in a wide range of oxidation states, we anticipate new chemistry of site-isolated Os atoms. We chose MgO as a support because it is excellent for imaging of heavy metal atoms on it[6] and has been shown to be a platform for site-isolated osmium complexes.[6c] Herein we report spectra, images, and theoretical electronic structure results characterizing stable new site-isolated complexes of osmium in various oxidation states and evidence of new reactivities and catalytic properties. CO and ethylene are ligands that are also intermediates in catalytic reactions that can be readily characterized by IR spectroscopy and DFT calculations. They were therefore used to probe the supported osmium species various conditions of treatment and catalysis.

We synthesized $Os(CO)_2$ on MgO powder, as before,[6c] characterizing the intermediate species spectroscopically and confirming earlier results; details are given in the Supporting Information (SI). IR spectra including pairs of ν_{CO} bands at 1981 and 1894 cm^{-1} and at 2012 and 1917 cm^{-1}, respectively (Figure S1 in SI) and extended X-ray absorption fine structure (EXAFS) spectra determine the structure,[6c] and STEM images demonstrate the site isolation of the Os atoms on various MgO faces.[6c, 8]

Table 1. EXAFS data at the Os L_{III} edge characterizing samples prepared by reaction of $Os_3(CO)_{12}$ with MgO after various treatments.[a]

Treatment conditions	Shell	*N*	EXAFS results[b] *R* (Å)	$10^3\times\Delta\sigma^2$ ($Å^2$)	ΔE_0 (eV)	DFT *R* (Å)
He, 548 K, 2 h	Os–Os	[c]	[c]	[c]	[c]	
	$Os–C_{CO}$	1.9	1.89	6.7	7.8	1.85
	$Os–O_{CO}$	1.9	3.23	5.3	-4.9	3.03
	$Os–O_{support}$	3.5	2.06	7.6	-3.7	2.19
	Os–Mg	4.4	3.05	4.6	-3.5	3.03
He, 548 K, 2 h, and 623 K, 2 h	Os–Os	[c]	[c]	[c]	[c]	
	Os=O	1.6	1.78	12.2	4.4	1.72
	$Os–O_{support}$	1.7	1.94	5.4	8.0	1.98
	Os–Mg	3.9	3.02	10.3	-1.8	
	$Os–O_{long}$	4.4	4.06	6.7	-0.39	

[a] Notation: *N*, coordination number; *R*, distance between absorber and backscatterer atoms; $\Delta\sigma^2$, variance in the absorber–backscatterer distance (Debye-Waller factor); ΔE_0, inner potential correction. Error bonds (accuracies) characterizing the structural parameters estimated to be *N*, ±20%; *R*, ±0.02 Å ; $\Delta\sigma^2$, ±20%; ΔE_0, ±20%. [b] EXAFS data for the sample treated at 548 K in He from ref [6c]; results for sample further treated at 623 K for 2 h, this work, with goodness of fit of 6.4. [c]Contribution not detectable. Details of EXAFS data fitting provided in SI.

Electronic structure calculations at the density functional theory level (DFT/B3LYP) were done to model the osmium dicarbonyls as a singlet cluster, $(MgO)_{24}OOs(II)(CO)_2$, with Os located at a Mg vacancy[6c, 8] and bonded to 4 O atoms (Figure 1, Model **a**). The structure agrees well with the EXAFS data (Table 1), and the calculated ν_{CO} frequencies, 2017 and 1935 cm^{-1}, are in good agreement with the experimental results when Os is bonded to 4 O atoms (2012 and 1917 cm^{-1}). To determine the identity of the other $Os(CO)_2$ species with the ν_{CO} bands at 1981 and 1894 cm^{-1} (Figure S1, SI), we calculated another cluster, $(MgO)_{16}Os(0)(CO)_2$, with the Os atom bridging two lattice O atoms (Figure 1, Model **b**). This model is characterized by a pair of CO bands, at 1983 and 1910 cm^{-1}, consistent with experiment. Thus, two types of bonding sites are inferred for the $Os(CO)_2$ species, corresponding to Models **a** and **b**.

[a] Dr. D. Yang, Dr. P. H. Xu, Prof. Dr. B. C. Gates
Department of Chemical Engineering and (formerly) Materials Science, University of California, Davis, California 95616, United States
E-mail: bcgates@ucdavis.edu (B.C.G.)
[b] S. J. Zhang, Prof. Dr. D. A. Dixon
Department of Chemistry, The University of Alabama, Shelby Hall, Box 87036, Tuscaloosa, AL 35487-0336, United States
E-mail: dadixon@ua.edu (D. A. D.)
[c] Prof. Dr. N. D. Browning
Physical and Computational Sciences, Pacific Northwest National Laboratory, 902 Battelle Boulevard, Richland, Washington 99352, United States
Email: Nigel.Browning@pnnl.gov (N. D. B.)

Supporting information for this article is given via a link at the end of the document.

WILEY-VCH

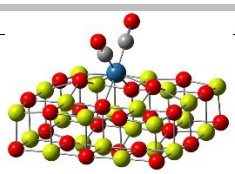

Model a, $(MgO)_{24}OOs(II)(CO)_2$ (the Os is in the lattice)

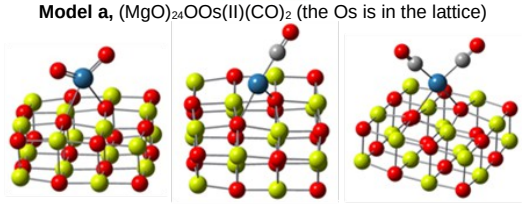

Model b. $[(MgO)_{16}Os(O)_2]^{m+}$, $[(MgO)_{16}Os(CO)]^{m+}$, $[(MgO)_{16}Os(CO)_2]^{m+}$ (m = 0 or 2)

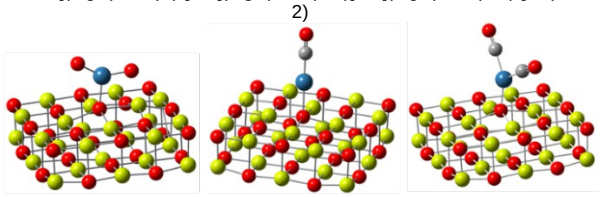

Model c. $(MgO)_{25}Os(IV)(O)_2$, $(MgO)_{25}Os(0)(CO)$, and $(MgO)_{25}Os(0)(CO)_2$

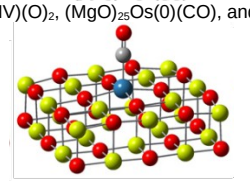

Model d. $[(MgO)_{24}Os(I)(CO)]^+$, $[(MgO)Os(II)(CO)]^{2+}$(the Os atom is in the lattice and the O atom underneath it is missing)

Figure 1. DFT models characterizing MgO-supported osmium species

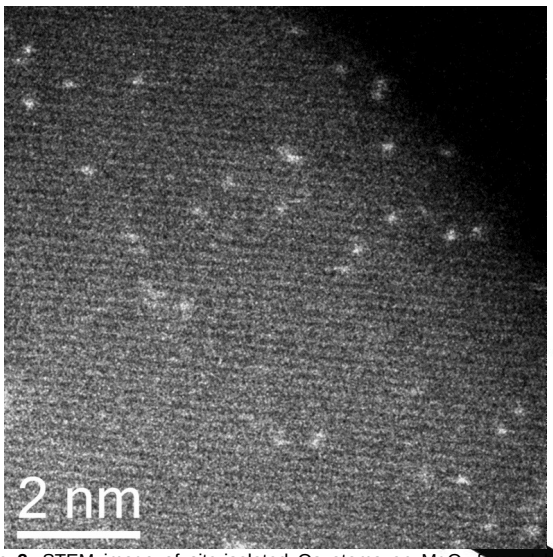

Figure 2. STEM image of site-isolated Os atoms on MgO, formed by the adsorption of $Os_3(CO)_{12}$ on MgO after treatment described in text. Image analysis shows that >90% of the Os atoms are clearly site-isolated, with <10% close enough together (within 2.9 Å) to suggest possible Os-Os bonding and hence dimers; the value of 10% is an upper limit because the neighbouring Os atoms could lie in different planes and be farther apart than the distance measured in the 2-dimensional image.

Heretofore, investigations of the chemistry of supported osmium complexes have been stymied by the challenge of replacing the tightly bonded CO ligands without aggregation of the osmium,[9] but we discovered how to remove these ligands without osmium aggregation, by treatment in flowing helium with the temperature ramped from 298 to 623 K and held for 2 h. IR (Figure S1, SI). EXAFS spectra (Table 1) demonstrate that all the CO ligands were removed and that each isolated Os atom became bonded, on average, to 1 or 2 O atoms of the MgO, with no evidence of Os–Os contributions that would indicate osmium clusters (Table 1). STEM images (Figures 2 and S2, SI) demonstrate that the Os atoms were site isolated before and after decarbonylation and also (Figure S3, SI) that the Os atoms on the MgO(110) face were located directly on top of Mg atomic columns after decarbonylation as well as before.

The X-ray absorption data characterizing the decarbonylated sample indicate oxidation of the osmium during decarbonylation. An Os–O contribution with a coordination number (*CN*) of 1.6 ± 0.3 at an average distance of 1.78 ± 0.02 Å (much less than the $Os–O_{support}$ bonding distance of about 1.94 Å) indicates mononuclear osmium oxide species on the support. Comparison of the shorter Os–O distance with the Os=O bond distance in OsO_4 (1.72 Å[10]) points to osmium oxo species. The EXAFS data further indicate Os–support contributions that were fitted with $Os–O_{support}$ and Os–Mg shells, the former with a *CN* of 1.7 ± 0.3 at an average distance of 1.94 Å and the latter (which the data determine with less confidence) with a *CN* of 3.9 ± 0.8 at an average distance of 3.02 Å. Because these results demonstrate bonding of the osmium oxo complexes to the support through one or two $Os–O_{support}$ bonds, we represent the surface species as $Os(=O)_{1or2}\{–O_{support}\}_{1or2}$.

Mass spectra of the effluent gas formed during decarbonylation of the supported osmium carbonyl in a flow system indicate H_2 (*m/z* = 2) and CH_4 (*m/z* = 15) as major products (Figure S4, SI), whereas no CO (*m/z* = 28) or CO_2 (*m/z* = 44) was observed. We did not observe any *m/z* = 2 or *m/z* = 15 signals for bare MgO (that had been soaked in pentane for 1 day; pentane was thereafter removed by exposure to high vacuum for 1 day). Thus, we infer that the chemistry of CO removal involves the breaking of $Mg–O_{support}$ bonds, the formation of Os=O bonds, and reduction of support OH groups to give H_2 which reacted with CO to form CH_4, possibly catalyzed by the osmium centers. XANES data (Figure S5, SI) show that the Os L_{III} white line intensity increased during the decarbonylation, confirming oxidation of the osmium.

Because the $Os–O_{support}$ coordination number of 1.7 (an average over the whole sample) is too low for a structure in which an Os atom is bonded at an Mg vacancy on MgO,[6c, 8] we infer that the Os atoms moved from vacancy sites on the MgO surface during the oxidative treatment. DFT calculations were done to elucidate details of the chemistry of the various surface species, as summarized in the SI. The $Os–O_{support}$ coordination number of 1.7 is consistent with the inference that structures similar to Models **b** and **c** (Figure 1) coexist in the sample, which we represent as a mixture, $Os(=O)_2\{–O_{support}\}_{1or2}$. Because the bonding distances of $Os–O_{support}$ and Os=O in Model **c**, $(MgO)_{25}Os(IV)(O)_2$ (1.98, 1.71 Å), and Model **b**, $[(MgO)_{16}Os(VI)(O)_2]^{2+}$ (1.96, 1.69 Å) are closer to the EXAFS results (1.94, 1.78 Å) than the others (Model **b** with charge 0 or 1+), we suggest that these two are the majority species. We emphasize that Model **c** is consistent with the images showing Os atoms on top of Mg columns on the MgO(110) face. DFT calcuations also show that the two models are both energetically favored and indicate the oxidation was formally of Os(0) (Model **b** with charge 0) and Os(II) (Model **a**) dicarbonyl complexes to Os(IV) (Model **c**) and Os(VI) (Model **b** with charge 2+) dioxo species.

Atomic populations were determined using NBO6[11] for the natural bond orbital (NBO)[12] population analysis at the DFT level. For the $Mg_{24}O_{25}Os$ model **a** where Os has replaced an Mg in the lattice, the loss of CO leads to a more positive Os atom in the +II oxidation state, whereas the removal of CO followed by oxidation with O_2 leads to a significantly more positive Os atom by 0.64 eV for the formal +IV oxidation state. Removal of CO from the Os(IV) atom also leads to a significant change in the Os

WILEY-VCH

charge for the bare Os atom or for the addition of O_2 to the Os atom. In Model **c**, the Os atom is on top of an O atom in the cluster. Loss of CO from the Os(0) leads to an increase in charge on the Os atom and an even greater increase in charge by 1.38 eV on the Os atom when it is further oxidized by O_2. For model **b**, the Os atom bridges two O atoms in the cluster. Loss of CO from the Os(0) atom leads to an increase in charge on the Os and an even greater increase in charge by 1.36 eV on the Os atom when it is further oxidized by O_2. The results are completely consistent with the XANES result which show that the Os becomes more positive as a result of removal of the CO ligand.

The reactivity of the site-isolated osmium oxo complexes was probed with $^{12}C_2H_4$ pulsed into a helium stream (80 $^{12}C_2H_4$ molecules/Os atom) flowing steadily into an IR cell with the sample at 1 bar and 298 K. Bands appeared at 2924 and 2850 cm^{-1} in the C–H stretching region and at 1047 cm^{-1} in the C–O region (Figure S6, SI). When $^{12}C_2H_4$ was replaced with $^{13}C_2H_4$, these bands were red-shifted to 2916, 2844, and 1026 cm^{-1}, respectively, demonstrating the formation of what we infer to be an osmium glycol species formulated as $Os(OCH_2CH_2O)$.[13] The inference is based on the spectrum of the Os(VI) di-ester $OsO(OCH_2CH_2O)_2$ formed by the reaction of OsO_4 with ethylene, which has a C–O band at 1016 cm^{-1} and C–H bands between 2850 and 2900 cm^{-1} (the frequency of the C–O band is strongly influenced by the ligands on the osmium (e.g., that representing $OsO_2(C_2H_5N)_2(OCH_2CH_2O)$ is located at 1041 cm^{-1} [5, 13]). Thus, the reactivity of supported $Os(=O)_2$ is inferred to be analogous to that of OsO_4 in forming the oxoosmium(VI) ester—a key structure in Sharpless' asymmetric dehydroxylation chemistry,[13] whereby this compound reacts further to generate diol products with the involvement of water and an oxidant.[5, 14]

We calculated the energetics of the reaction of C_2H_4 with the Os(IV) (Model **c**) and Os(VI) (Model **b** with charge 2+) to generate Os(II) and Os(VI) sites with glyoxalate, finding the reactions to be exothermic by -27 and -14 kcal/mol, respectively. Thus, we infer that the species that reacts with ethylene is Model **b (**Os(VI)), which readily forms $Os(OCH_2CH_2O)$. The calculated frequencies for glyoxal formed from Model **b** Os(VI) match experiment. An essential point is that there is not a single model of the surface species that agrees well with experiment—rather the results point to a mixture of surface species.

To provide more information about the surface $Os(=O)_2$ species, we allowed CO to flow over the sample in an IR cell at 1 bar and temperatures lower than 473 K. These temperatures were chosen to avoid the formation of clusters of osmium atoms; we emphasize that the temperatures were much lower than the temperatures applied to generate osmium oxo complexes. At temperatures less than 393 K, essentially no changes in the ν_{CO} region of the spectrum ensued, but at 473 K, reaction occurred, evidenced by CO_2 found by mass spectrometry in the effluent stream. Simultaneously, six new bands gradually appeared in the ν_{CO} region of the spectra, centered at 1894, 1914, 1938, 1960, 1981, and 2012 cm^{-1} (Figure S7, SI). No shifts of these bands were observed as they grew in. When the treatment gas was ^{13}CO, the bands appeared at 1848, 1866, 1893, 1913, 1927, and 1958 cm^{-1} (Figure S8, SI), and the frequencies and shifts of these bands, consistent with the harmonic approximation, show that they represent osmium carbonyls. We assign the bands at 2012, 1981, and 1894 cm^{-1} to the two Os(II) dicarbonyl species bonded to 4 or 2 support oxygen atoms, because the frequencies match those shown in Figure S1 in the SI. We infer that no osmium clusters formed during the CO treatment or the later CO/O_2 treatment, because we observed no bridging carbonyl bands in the IR spectra (which would have been expected for osmium clusters at approximately 1800 cm^{-1}) and because the literature[15] demonstrates that under conditions similar to ours, CO is a reactant that oxidatively fragments noble metal clusters on oxide supports.

When, after the carbonylation, the temperature was decreased to 298 K and the gas stream switched to $^{12}C_2H_4$, no IR bands characteristic of esters were detected, implying the complete removal of the $Os(=O)_2$ species. Thus, we infer that the MgO-supported complex $Os(=O)_2\{-O_{support}\}_{1or2}$ was reduced by CO at 473 K.

Table 2. Assignments of the carbonyl bands observed in this work

Species	Number of support oxygen atoms bonded to Os	Frequencies, cm^{-1}, experimental	Frequencies, cm^{-1}, DFT calculated
$Os^{2+}(CO)_2$	2	1981, 1894	1983, 1910, Model **b**
$Os^{2+}(CO)_2$	4	2012, 1917	2017, 1935, Model **a**
$Os^{2+}(CO)$ or $Os^0(CO)$	4 or 2	1914~1917	1922, Model **d**, or 1907, Model **b**
$Os^{2+}(CO)$	4	1935~1942	1932, Model **d**
$Os^0(CO)$	1	1960~1968	1966, Model **c**

The bands at 1914, 1938, and 1960 cm^{-1} are all lower in frequency than the symmetric bands characterizing Os(II) dicarbonyl (2012 or 1981 cm^{-1}), implying that they do not represent any osmium dicarbonyls, and consequently we suggest that they represent osmium monocarbonyls. To clarify the chemistry, DFT calculations were done for several supported osmium monocarbonyls with various modes of bonding to support oxygen. The calculated scaled ν_{CO} values characterizing $(MgO)_{24}Os(0)(CO)$ (Model **b**), $[^2Mg_{24}O_{24}Os(I)(CO)]^+$ (Model **d**), $[^1Mg_{24}O_{24}Os(II)(CO)]^{2+}$ (Model **d**), and $^3(MgO)_{25}Os(0)(CO)$ (Model **c**) are 1907 (1361 km/mol), 1922 (871 km/mol), 1932 (980 km/mol), and 1966 (1521 km/mol) cm^{-1}, respectively, matching the experimental observations within ±8 cm^{-1}. Thus, we assign the bands observed at 1914, 1938, and 1960 cm^{-1} to CO ligands of monocarbonyls of isolated Os atoms with different charges and in different sites. A summary of the assignments of all the carbonyl bands is presented in Table 2.

The reactivities of these supported osmium carbonyls with O_2 were investigated with a flow reactor at 473 K. When O_2 flowed steadily through the IR cell containing the sample, CO_2 was detected in the effluent by mass spectrometry (Figure S9, SI). Figures 3 and S10 (SI) show that the osmium monocarbonyl bands at 1914, 1938, and 1960 cm^{-1} decreased rapidly in intensity and in proportion to each other, indicating that the species they represent reacted with O_2. At the conclusion of a 22-min reaction period, these three osmium monocarbonyl bands had shifted to 1917, 1942, and 1966 cm^{-1}, respectively, as a result of the reaction with O_2. In contrast, the bands representing the osmium dicarbonyl species at 1894, 1981, and 2012 cm^{-1} did not change, indicating the lack of reactivity of this species with O_2. Because the band at 1914 cm^{-1} decreased substantially in intensity under these treatment conditions (remaining in the narrow range of 1914-1917 cm^{-1}), we infer that it represents a species ($Os^{2+}(CO)$ or $Os^0(CO)$,) different from that represented by the band observed at 2012 cm^{-1} ($Os^{2+}(CO)_2$). We infer that the catalytic CO oxidation reaction requires the bonding of both CO and oxygen to single Os centers. The bonding of CO to osmium species is evidenced by the carbonyl

bands in the IR spectra, and the bonding of oxygen by the shift of the carbonyl bands to higher frequencies after contact of the sample with O_2. The data show that only those species with ν_{CO} bands that shift to higher frequencies in O_2 (osmium monocarbonyls) react with O_2. The Os(II) dicarbonyl species were unreactive, presumably because the adsorption of O_2 was blocked by the CO ligands.

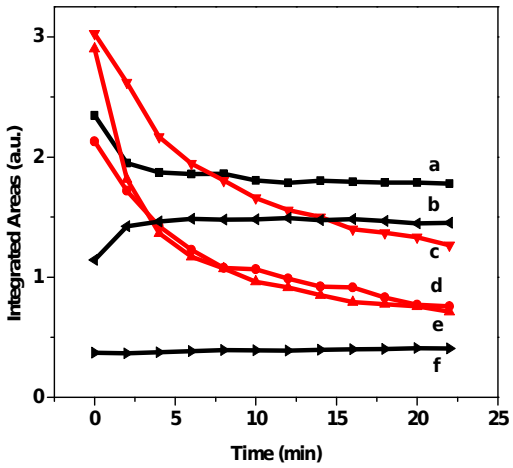

Figure 3. Integrated area changes of IR bands in C–O stretching region characterizing the sample made from $[Os_3(CO)_{12}$ on MgO after contact with flowing O_2 for 23 min at 473 K. The initially prepared sample was treated in flowing helium at 548 K for 2 h and at 623 K for 2 h, followed by CO adsorption at 473 K for 20 min, then helium flow for 30 min. Data are shown for the following bands (cm^{-1}): a, 1894; b, 1981; c, 1960; d, 1914; e, 1938; and f, 2012.

We tested the supported sample initially in the form of $Os(=O)_2\{–O_{support}\}_{1or2}$ for CO oxidation catalysis in a plug-flow reactor at 473 K at CO and O_2 partial pressures of 10 mbar each. The initial activity (turnover frequency, *TOF*) was less than 10^{-4} (molecules of CO)/(Os atom × s), but the *TOF* gradually increased with time on stream and stabilized at a value of 4.0×10^{-3} (Figure S11, SI). Osmium dicarbonyls with IR bands at 2012, 1981, and 1894 cm^{-1} and osmium monocarbonyl species characterized by IR bands at 1968 and 1935 cm^{-1} (Table 2) formed during the catalysis (Figure S12, SI). Slight shifts of the osmium monocarbonyl bands at 1968 and 1935 cm^{-1} from those initially observed at 1963 and 1931 cm^{-1} took place (Figure S12, SI) because CO and O_2 were present together in the gas—indicative of the interactions of more than one species with osmium monocarbonyls, but we do not exclude a possible role of MgO in the chemistry. In contrast, the osmium dicarbonyl bands at 2012, 1981, and 1894 cm^{-1} remained unchanged in frequency, indicating the lack of reactivity of this species with CO and O_2 together—and so we infer that not the osmium dicarbonyls but rather the osmium monocarbonyls (with bands at 1968 and 1935 cm^{-1}) are the catalytically active species. Because no carbonyl bands were observed to arise in the spectrum of the $Os(=O)_2\{–O_{support}\}_{1or2}$ present initially, we suggest that the adsorption of CO was blocked by the oxygen ligands, leading to the low catalytic activity of this sample for CO oxidation (*TOF* < 10^{-4}). We infer the increase of *TOF* in the first 20 min during CO oxidation catalysis (Figure S11, SI) is associated with the appearance of active osmium monocarbonyl species (with bands at 1968 and 1935 cm^{-1}, respectively, Figure S12, SI). For comparison, a *TOF* value was reported to be 1.3×10^{-2} with feed partial pressure of $CO:O_2$ = 1:1 at 473 K for a 0.4% Rh_1/O_v-supported single-site platinum catalyst[16] (the reaction conditions were similar to ours), three times higher than ours. We also tested the activty of the supported sample initially in the form of $Os(CO)_2\{–O_{support}\}_{2or4}$ for CO oxidation under similar conditions. The activity was also found to be very low (*TOF* < 10^{-4}), consistent with the inference that the active species are osmium mono- rather than di-carbonyls.

The spectra and images show that site isolation was maintained when the single-site supported $Os(CO)_2$ was oxidized to give $Os(=O)_2$. We emphasize that the removal of the CO ligands in this decarbonylation was not a simple ligand dissociation that left coordinatively unsaturated Os centers on the MgO. In general we do not expect to easily form coordinatively unsaturated site-isolated metal complexes on hydroxylated metal oxides, and there is a lack of evidence for any such species.

In summary, our results demonstrate the presence of osmium in various oxidation states in complexes of various structures and new surface chemistry related to Sharpless asymmetric dehydroxylation chemistry. The various single-site osmium species were used as CO oxidation catalysts, and the results show that only osmium monocarbonyl species were active for this reaction. The results determined with multiple complementary techniques, thus emphasize the complexity of the chemistry of metal complexes on metal oxide surfaces, and we posit that this complexity is a more general characteristic of oxide-supported single-site supported catalysts than has been recognized.

Acknowledgments

This work was supported by the U.S. Department of Energy (DOE), Office of Science, Basic Energy Sciences, Grant DE-FG02-04ER15513, and by the catalysis center program led by PNNL. A portion of this work was done as part of the Chemical Imaging Initiative at Pacific Northwest National Laboratory (PNNL) (under Contract DE-AC05-76RL01830), operated for DOE by Battelle. It was conducted under the Laboratory Directed Research and Development Program at PNNL. A portion of the research was performed at EMSL, a national scientific user facility sponsored by the DOE's Office of Biological and Environmental Research and located at PNNL. We acknowledge beam time at beamline 4-1 at the Stanford Synchrotron Radiation Lightsource supported by the DOE Division of Materials Sciences. We thank the beamline staff for valuable support.

Keywords: supported single-site catalyst • osmium • osmium oxo • carbonyl ligands • CO oxidation catalysis

[1] a) M. Flytzani-Stephanopoulos, B. C. Gates, *Annu. Rev. Chem. Biomol. Eng.* **2012**, *3*, 545-574.; b) X. G. Guo, G. Z. Fang, G. Li, H. Ma, H. J. Fan, L. Yu, C. Ma, X. Wu, D. H. Deng, M. M. Wei, D. L. Tan, R. Si, S. Zhang, J. Q. Li, L. T. Sun, Z. C. Tang, X. L. Pan, X. H. Bao, *Science* **2014**, *344*, 616-619; c) X. F. Yang, A. Q. Wang, B. T. Qiao, J. Li, J. Y. Liu, T. Zhang, *Acc. Chem. Res.* **2013**, *46*, 1740-1748.

[2] a) J. Guzman, B. C. Gates, *Angew. Chem. Int. Edit.* **2003**, *42*, 690-693; b) J. C. Fierro-Gonzalez, B. C. Gates, *J. Phys. Chem. B* **2004**, *108*, 16999-17002; c) M. Yang, S. Li, Y. Wang, J. A. Herron, Y. Xu, L. F. Allard, S. Lee, J. Huang, M. Mavrikakis, M. Flytzani-Stephanopoulos, *Science* **2014**, *346*, 1498-1501; d) M. Yang, L. F. Allard, M. Flytzani-Stephanopoulos, *J. Am. Chem. Soc.* **2013**, *135*, 3768-3771; e) B. T. Qiao, J. X. Liu, Y. G. Wang, Q. Q. Lin, X. Y. Liu, A. Q. Wang, J. Li, T.

Zhang, J. Y. Liu, *ACS Catal.* **2015**, *5*, 6249-6254; f) C. Y. Wang, M. Yang, M. Flytzani-Stephanopoulos, *AIChE J.* **2016**, *62*, 429-439.

[3] a) B. T. Qiao, A. Q. Wang, X. F. Yang, L. F. Allard, Z. Jiang, Y. T. Cui, J. Y. Liu, J. Li, T. Zhang, *Nat. Chem.* **2011**, *3*, 634-641; b) J. D. Kistler, N. Chotigkrai;, P. Xu;, B. Enderle;, P. Praserthdam;, C. Y. Chen, N. D. Browning, B. C. Gates, *Angew. Chem. Int. Edit.* **2014**, *53*, 8904-8907; c) M. Yang, J. L. Liu, S. Lee, B. Zugic, J. Huang, L. F. Allard, M. Flytzani-Stephanopoulos, *J. Am. Chem. Soc.* **2015**, *137*, 3470-3473; d) H. S. Wei, X. Y. Liu, A. Q. Wang, L. L. Zhang, B. T. Qiao, X. F. Yang, Y. Q. Huang, S. Miao, J. Y. Liu, T. Zhang, *Nat. Commun.* **2014**, *5*, 5634/1-8.

[4] a) A. Uzun, V. A. Bhirud, P. W. Kletnieks, J. F. Haw, B. C. Gates, *J. Phys. Chem. C* **2007**, *111*, 15064-15073; b) J. Lin, A. Q. Wang, B. T. Qiao, X. Y. Liu, X. F. Yang, X. D. Wang, J. X. Liang, J. X. Li, J. Y. Liu, T. Zhang, *J. Am. Chem. Soc.* **2013**, *135*, 15314-15317.

[5] H. C. Kolb, M. S. Vannieuwenhze, K. B. Sharpless, *Chem. Rev.* **1994**, *94*, 2483-2547.

[6] a) A. Uzun, V. Ortalan, N. D. Browning, B. C. Gates, *J. Catal.* **2010**, *269*, 318-328; ; b) A. Uzun, V. Ortalan, Y. Hao, N. D. Browning, B. C. Gates, *J. Phys. Chem. C* **2009**, *113*, 16847-16849; c) C. Aydin, A. Kulkarni, M. F. Chi, N. D. Browning, B. C. Gates, *J. Phys. Chem. Lett.* **2012**, *3*, 1865-1871.

[7] a) V. A. Bhirud, H. Iddir, N. D. Browning, B. C. Gates, *J. Phys. Chem. B* **2005**, *109*, 12738-12741; b) R. Psaro, C. Dossi, R. Ugo, *J. Mol. Catal.* **1983**, *21*, 331-351; c) S. Mehraeen, A. Kulkarni, M. F. Chi, B. W. Reed, N. L. Okamoto, N. D. Browning, B. C. Gates, *Chem. Eur. J.* **2011**, *17*, 1000-1008; d) A. Kulkarni, M. F. Chi, V. Ortalan, N. D. Browning, B. C. Gates, *Angew. Chem. Int. Edit.* **2010**, *49*, 10089-10092.

[8] O. Alexeev, B. C. Gates, *Top. Catal.* **2000**, *10*, 273-293.

[9] C. Aydin, A. Kulkarni, M. F. Chi, N. D. Browning, B. C. Gates, *Angew. Chem. Int. Edit.* **2013**, *52*, 5262-5265.

[10] W. P. Griffith, *Plat. Met. Rev.* **1974**, *18*, 94-96.

[11] a) E. D. Glendening, J. K. Badenhoop, A. E. Reed, J. E. Carpenter, J. A. Bohmann, C. M. Morales, C. R. Landis, F. Weinhold, Theoretical Chemistry Institute, University of Wisconsin, Madison, WI, **2013**; b) E. D. Glendening, C. R. Landis, F. Weinhold, *J. Comp. Chem.* **2013**, *34*, 1429-1437.

[12] a) F. Weinhold, In Encyclopedia of Computational Chemistry; P. V. R. Schleyer, Ed.; John Wiley & Sons: Chichester, U.K. **1998**, *3*, 1792−1811; b) F. Weinhold, C. R. Landis, Valency and Bonding: A Natural Bond Orbital Donor-Acceptor Perspectiv[illegible] University Press: Cambridge, U.K. **2003**; c) A. E. Reed, L. A. Curtiss, F. W[illegible]nhold, *Chem. Rev.* **1988**, *88*, 899-926; d) A. E. Reed, R. B. Weinstock, F. [illegible]nhold, *J. Chem. Phys.* **1985**, *83*, 735-746.

[13] R. J. Collin, J. Jones, W. P. Griffith, *J. Chem. Soc. Dalton Trans.* **1974**, 1094-1097.

[14] W. P. Griffith, R. Rossetti, *J. Chem. Soc. Dalton Trans.* **1972**, 1449-1453.

[15] a) A. Suzuki, Y. Inada, A. Yamaguchi, T. Chihara, M. Yuasa, M. Nomura, Y. Iwasawa, *Angew. Chem. Int. Ed.* **2003**, *42*, 4795-4799; b) A. Berko, G. Menesi, F. Solymosi, *J. Phys. Chem.* **1996**, *100*, 17732-17734; c) A. Berko, F. Solymosi, *J. Catal.* **1999**, *183*, 91-101; d) D. Tang, P. H. Xu, E. J. Guan, N. D. Browning, B. C. Gates, *J. Catal.* **2013**, *338*, 12-20; e) P. Serna, D. Yardimci, J. D. Kistler, C. C. Gates, *Phys. Chem. Chem. Phys.* **2014**, *16*, 1262-1270.

[16] M. Moses-DeBusk, M. Yoon, L. F. Allard, D. R. Mullins, Z. L. Wu, X. F. Yang, G. Veith, G. M. Stocks, C. K. Narula, *J. Am. Chem. Soc.* **2013**, *135*, 12634-12645.

WILEY-VCH

Table of Contents

COMMUNICATION

Chemistry of MgO-supported single-site osmium complexes and catalysis of CO oxidation

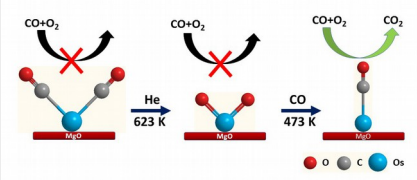

Dong Yang, Shengjie Zhang, Pinghong Xu, Nigel D. Browning, David A. Dixon, Bruce C. Gates**

Page No.1 – Page No.6

Single-site osmium catalysts on MgO: reactivity, and catalysis of CO oxidation